Malaysian Journal of Analytical Sciences
(MJAS)
Published by Malaysian Analytical Sciences Society
ANALIS
Persatuan Sains Analisis Malaysia

CORROSION BEHAVIOR OF LOW-CARBON STEEL AND STAINLESS STEEL 304 UNDER TWO SOIL CONDITIONS AT PANTAI MENGABANG TELIPOT, TERENGGANU, MALAYSIA

(Kelakuan Kakisan dan Penyusutan Bahan Logam Rendah Karbon dan Keluli Tahan Karat 304 di dalam Dua Keadaan Tanih di Pantai Mengabang Telipot, Terengganu, Malaysia)

Suriani Mat Jusoh[1, 2], Wan Mohd Norsani Wan Nik[1, 3, 4], Nor Azila Azman[1],
Mohammad Fakhratul Ridwan Zulkifli[1,3]*

[1]*Faculty of Ocean Engineering Technology and Informatics*
[2]*Composite Research Group (CoReG), Faculty of Ocean Engineering Technology and Informatics*
[3]*Materials and Corrosion Research Group, Faculty of Ocean Engineering Technology and Informatics*
[4]*Industrial Centre of Excellent (ICoE)*
Universiti Malaysia Terengganu, 21030 Kuala Nerus, Terengganu, Malaysia

**Corresponding author: fakhratulz@umt.edu.my*

Received: 14 June 2020; Accepted: 11 September 2020; Published: xx December 2020

Abstract

Corrosion damage significantly affect steel structures' performance, whose control is a crucial key for design and maintenance. In this study, two different steels' corrosion behaviour, namely as low-carbon steel (LCS) and stainless steel 304 (SS 304) strip coupons, were observed in two different soils for a maximum period of 56 days. The corrosion behaviour of buried metals in different soils was characterized by weight loss (WL) measurement, potentiodynamic polarization (PP), electrochemical impedance spectroscopy (EIS), and scanning electron microscopy (SEM). The results show that the average weight loss after the observational periods of 14,28,42 and 56 days, average percentage weight loss in the LCS coupons from the sandy soil site was 0.444%, 0.831%, 2.542%, and 3.084%, respectively, representing an overall average of 6.901%. The average percentage of weight loss was 0.761%, 1.770%, 2.833%, and 5.090%, respectively, representing an overall average of 10.454% in the silt soil. Corrosion rates (CRs) for the LCS coupons from sandy soil site after 14, 28, 42, and 56 days were 0.87 mmpy, 0.80 mmpy, 1.67 mmpy and 1.54 mmpy respectively. In the silt soil, the CRs were 1.47 mmpy, 1.74 mmpy, 1.87 mmpy and 2.56 mmpy. The value of E_{corr}, shifted to more negative values with increasing soil moisture content, indicating a cathodic controlled process. Moisture content is the most influential factor in metal loss, whereas pH is relatively insignificant in underground corrosion. Also, the pits area and distribution depend on the soil conditions. The corroded area of LCS was more extensive than the SS 304, where the depth of the pitting was the same across the surface.

Keywords: corrosion, materials, materials degradation, materials selection, scanning electron microcopy

Abstrak

Kerosakan kakisan sangat mempengaruhi prestasi struktur keluli, yang kawalannya adalah aspek utama reka bentuk dan penyelenggaraan. Dalam kajian ini, kelakuan kakisan dari dua jenis keluli berbeza iaitu keluli karbon rendah (LCS) dan keluli tahan karat 304 (SS 304) kupon jalur telah dinilai di dalam dua tanah yang berlainan untuk tempoh maksimum 56 hari. Pencirian produk kakisan telah dijalankan dengan menggunakan teknik pengurangan berat (WL), pengutuban keupayaan dinamik (PP), pengukuran spektroskopi impedans elektrokimia (EIS) dan imbasan elektron mikroskopi (SEM). Keputusan menunjukkan bahawa purata berat selepas tempoh pemerhatian 14, 28, 42 dan 56 hari, purata kehilangan berat dalam kupon LCS dari tapak tanah berpasir adalah 0.444%, 0.831%, 2.542% dan 3.084 %, mewakili purata keseluruhan sebanyak 6.901%. Di dalam tanah lumpur, purata kehilangan berat adalah 0.761%, 1.770%, 2.833% dan 5.090% mewakili purata keseluruhan 10.454%. Kadar kakisan untuk kupon LCS dari tanah berpasir selepas 14,28,42 dan 56 hari adalah 0.87 mmpy, 0.80 mmpy, 1.67 mmpy dan 1.54 mmpy, masing-masing memberikan purata komposit 1.22 mmpy. Di dalam tanah lumpur, CRs ialah 1.47 mmpy, 1.74 mmpy, 1.87 mmpy dan 2.56 mewakili purata 1.91 mmpy. Nilai E_{corr}, mengarah kepada lebih negatif dengan pertambahan kandungan kelembapan tanah menandakan proses kawalan katodik. Kandungan lembapan adalah faktor yang paling berpengaruh terhadap kehilangan logam, sedangkan pH secara relatif tidak ketara pada kakisan bawah tanah. Juga, kawasan lubang dan pengedaran juga bergantung kepada keadaan tanah. Kawasan berlubang pada logam LCS lebih besar berbanding SS 304 dan kedalaman lubang adalah sama.

Kata kunci: kakisan, bahan, penyusutan bahan, pemilihan bahan, imbasan mikroskop elektron.

Introduction

Soil corrosion problems can also be distinctive due to the difference in soil salt content, oxygen content, temperature and microbial species in various soils [1]. Soil corrosion is an essential factor that threatens the safe operation of the pipeline and is also the fundamental cause of pipeline corrosion failure [2, 3]. Observations and data derived from coupon testing have been used to determine the average rate of corrosion and the type of corrosion during the exposure interval. Corrosion rate data derived from a single exposure generally do not provide information on corrosion rate change versus time. Corrosion rate may increase, decrease, or remain constant, depending on the corrosion samples' nature and soil conditions [4]. Therefore, in this study, the corrosion behaviour and materials degradation of two metals type known as low-carbon steel and stainless steel 304 under two soil conditions were determined by different techniques such as electrochemical impedance spectroscopy (EIS), weight loss (WL) measurement and scanning electron microscopy (SEM).

Materials and Methods

Materials

Metal coupons of two metallurgies were used for this study provided by two companies (Visco Chemicals, Houston and Rohrback Cosasco Systems). They are low-carbon steel (LCS) coupons and stainless steel 304 (SS 304) coupons. Bar/strip style coupons were used in this study. The composition of LCS and SS304 are tabulated in Table 1 [5].

Sample preparation

All coupon types were cut (38 mm x 25 mm x 3mm) uniformly. The LCS and SS 304 coupon density is 7.85 g/cm^3 and 7.98 g/cm^3, respectively. There was no pre-treatment of the coupons before exposure to the soil sites and finally, the coupons were buried in a depth of 30 cm at both selected sites. Figure 1 shows both coupons after the surface preparation process.

Location

Two locations were selected to bury the test coupons (Kampung Tanjung Gelam and Kampung Gong Pak Jin). Both locations are situated nearby the beach area of Pantai Mengabang Telipot, Terengganu, Malaysia. All coupons were buried in duplicates in a depth of 30 cm at both the selected site of sandy soil and silt soil site, as depicted in Figures 2 and 3, respectively. Both selected sites randomly choose based on their properties and colour of the soil.

Weight loss and corrosion rate determination

The metal coupons were buried in the soil environments for a maximum of 56 days. For 14 days, 28 days, 42 days and 56 days, duplicate sets of the buried coupons in both sites were retrieved for analysis. On completion of every exposure experiment, the coupons were removed from the soil chamber and weight loss measurement was performed. Three coupons for each type of steels were taken out from a chamber, as depicted in Figure 4.

The buried coupon was monitored to determine the corrosion effect occurred on the coupon at the end of each observation period and to compare the effect corrosion rates in two different soil environments. Equation 1 was used to calculate the weight loss of the steel after the exposure. Total weight is the summation of initial weight (W_o) and final weight (W_f), as shown below [6].

$$\% \, Weight \; losss = \frac{W_f - W_o}{Wf} \times 100\% \tag{1}$$

The corrosion rate was calculated, assuming uniform corrosion over the entire surface of the coupons. The corrosion rate in mils per year (mmpy) was calculated from the weight loss using the formula in Equation 2 below:

$$CRs = \frac{W}{(DAT)} \times k \tag{2}$$

where: W = weight loss in gram, k = constant, D = metal density in g/cm^3, A = coupon area (cm^2) and t = time (hours).

Electrochemical impedance spectroscopy

The electrochemical impedance spectroscopy (EIS) test was performed by using Autolab PGSTAT 302N with three electrodes system. Rectangular coupons of mild steel and stainless steel were used as the working electrode. A platinum sheet was used as the auxiliary electrode and a saturated calomel electrode (SCE) was used as a reference electrode. An AC disturbance signal of 1 mV was applied on the electrode at the open circuit potential (OCP), while the measured frequency ranged from 0.01 to 105 Hz. All the electrochemical measurements were done twice at (25±1ºC). The potentiodynamic polarization curve measurement was collected at a scan rate of 5mV/s between -1.5V and +0.5V relative to the SCE.

Scanning electron microscopy

Scanning electron microscopy (SEM) was deployed to observe and analyze the morphology of the metal's surface. The experiment was conducted at the Institute of Oceanography (INOS) by using JEOL JSM-6390LA microscope model. The samples were subjected to a coating process with an ultrathin gold particle layer using JFC-1600 Auto Fine Coater (JEOL Ltd., Tokyo, Japan). The gold coated samples being electrically conductive allows for the scanning process on the sample surface at an accelerated voltage of 15 kV and a working distance of 10 mm [7]. SEM test was done after 28 days and 56 days of exposure to the soil.

Table 1. Composition of LCS and SS 304 in wt.%

Metal	**C**	**Si**	**Mn**	**S**	**P**	**Cr**	**Ni**	**Mo**	**Nb**	**Fe**
LCS	0.12	0.011	0.6	0.045	0.045	0.008	0.035	2-3	0.098	Bal
SS304	0.07	0.75	2.0	0.03	0.04	19	10	0.03	0.01	Bal

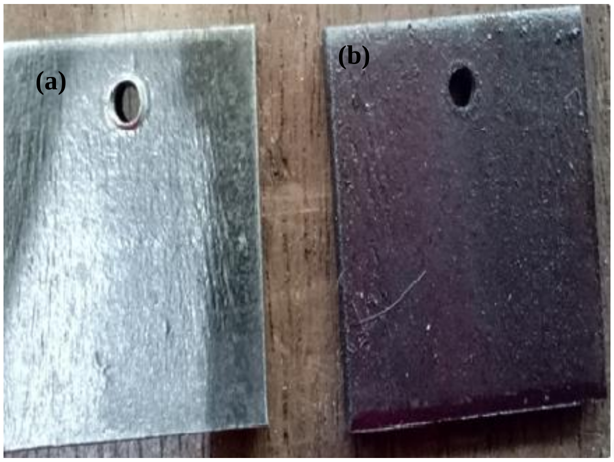

Figure 1. (a) Low carbon steel coupons and (b) Stainless steel 304 coupons

Figure 2. Sandy soil site at Kampung Tanjung Gelam, Mengabang Telipot.

Figure 3. Silt soil site at Kampung Gong Pak Jin, Mengabang Telipot

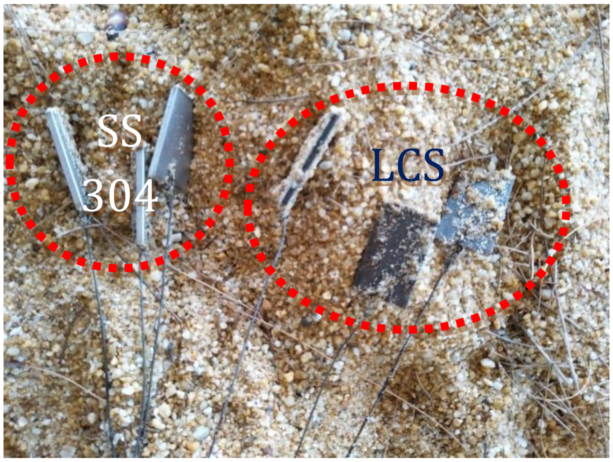

Figure 4. Three coupons for each steel taken out from a chamber.

Results and Discussion

Weight loss and corrosion rates

LCS and SS 304 coupons were buried in sandy soil and silt soil, where the condition of the two soils is different due to the moisture, pH, and temperature of the soil. Table 2 shows the value of weight loss of the studied metals, pH, temperature, and moisture content of the soils. The weight loss data was used to calculate the percentage of weight loss by using Equation 1.

The obtained weight loss data were used to determine the corrosion rates of LCS and SS304 relative to its exposure period by using Equation 2. The average corrosion rate of both coupons is tabulated in Table 3. According to the exposure period of 14, 28, 42 and 56 days, the weight loss percentage for- LCS coupons from the sandy soil site was 0.444%, 0.831%, 2.542%, and 3.084%, respectively, representing an overall average of 6.901% as depicted in Figure 5. In the silt soil site, the average percentage of weight loss was 0.761%, 1.770%, 2.833% and 5.090%, respectively, representing an overall average of 10.454%. It was found that both soil types show an increment of weight loss percentage due to the corrosion process. However, silt soil shows a higher average value of weight loss in comparison to the sandy soil.

At 14, 28, 42 and 56 days of exposure, the corrosion rates for the LCS from sandy soil were 0.87 mmpy, 0.80 mmpy, 1.67 mmpy and 1.54 mmpy, respectively, giving a total average of 1.22 mmpy. In the silt soil, the corrosion rates were 1.47 mmpy, 1.74 mmpy, 1.87 mmpy and 2.56 mmpy, respectively, representing an average of 1.91 mmpy as shown in Figure 6. As the corrosion rate's value is directly proportional to the percentage of weight loss, the trend for corrosion rate was found to be similar to the weight loss percentage trend.

In the sandy soil site, weight loss percentage for SS 304 coupons were 0.069%, 0.039%, 0.076% and 0.118% after 14.28,42 and 56 day respectively, with a total average of 0.076%, while the weight loss percentage in the silt soil were 0.035%, 0.055%, 0.118% and 0.165%, respectively, for combined average of 0.093%. Here, we see a near-similar increasing pattern as noted earlier, except for the dips on day 28 at both sites, as depicted in Figure 7. SS304 coupons show lower weight loss percentage due to its higher corrosion resistance nature as published by Anwar et al. (2017) in their study on the corrosion rate of SS304 and SS310 alloys in atmospheric, underground and seawater splash zone in the Arabian Gulf. It was determined that the corrosion rate for both SS304 and SS316 exposed under atmospheric, underground and seawater splash zone conditions is low due to higher corrosion resistance [8]. However, silt soil still gave a significant factor in weight loss percentage as it shows a higher weight loss percentage for SS304 compared with the coupons in sandy soil. Once again, moisture has become a major factor in exhibiting this trend. A slight difference in the percentage of weight loss and the corrosion rate for LCS at 42 days could be attributed to the anodic reaction rate. The anodic dissolution was decreased due to the accumulation of corrosion products on the metal surfaces. A similar finding was also reported elsewhere [9].

Corrosion rates for the SS 304 coupons from the sandy soil site were 0.15 mmpy, 0.04 mmpy, 0.06 mmpy and 0.07 mmpy after 14, 28, 42 and 56 days, with a cumulative average of 0.08 mmpy. For the silt soil sites, corrosion rates were 0.08 mmpy, 0.06 mmpy, 0.08 mmpy and 0.09 mmpy, respectively, for a cumulative average of 0.08 mmpy in Figure 8. The corrosion rate for SS304 was found to be lower than LCS due to its better corrosion resistance. The observed pattern for SS 304 in silt soil is higher than sandy soil due to more significant moisture content in this type of soil. However, after 14 days of exposure, the percentage of weight loss and corrosion rate for SS304 were higher in the sandy soil than silt soil. This is due to the susceptibility of SS304 towards localized corrosion compared to LCS, which generally exhibits uniform corrosion [10]. Localized corrosion could be enhanced by the chloride ion concentration in which sandy soil will entrap more chloride caused by marine aerosol. The trend was found to be inversed after 14 days and remained throughout the exposure period due to the corrosion mechanism's uniformity.

The findings found that the silt soil has prominent effects on weight loss and corrosion rate. This is due to the higher value of moisture found in silt soil, which figuratively double than the sandy soil. The presence of moisture enhances the ignition of the corrosion process as moisture is a prominent factor in the corrosion process. Moisture can create a thin layer of electrolyte and tend to suppress the formation of rust on the metal surface. This is aligned with the result reported by Akkouche et al. [9], where the authors stated that soil moisture is generally considered the most influential parameter because it strongly affects the most crucial point, which is the transport of oxygen (O_2) from the atmosphere to the steel surface. O_2 was transported via convection of the gas phase, which available in partially filled pores. Silt soil has low porosity due to its smaller particles and minerals size, then O_2 permeability is higher than sandy soil. In general, soil moisture plays a vital role in controlling oxygen diffusion through soils, electrical conductivity, and ionic migration in soils as well as soil-metal interfacial characteristics, which consequently affects the corrosion process [11].

Table 2. Result of average metal loss and *in-situ* parameters

Soil type	**Coupon Type**	**Time (day)**	**Weight Loss (g)**	**pH**	**Temperature (°C)**	**Moisture Content (%)**
Sandy soil	LCS	14	0.164	7.0	32	7.5
		28	0.301	7.0	30	8.9
		42	0.939	7.0	28	3.3
		56	1.159	7.0	30	8.0
	SS 304	14	0.016	7.0	32	7.5
		28	0.024	7.0	30	8.9
		42	0.050	7.0	28	3.3
		56	0.071	7.0	30	8.0

Table 2 (cont'd). Result of average metal loss and *in-situ* parameters

Soil type	Coupon Type	Time (day)	Weight Loss (g)	pH	Temperature (°C)	Moisture Content (%)
Silt soil	LCS	14	0.276	6.1	24	17.7
		28	0.652	6.3	23	19.2
		42	1.055	6.3	25	16.9
		56	1.924	6.2	25	20.0
	SS 304	14	0.030	6.1	24	17.7
		28	0.017	6.3	23	19.2
		42	0.033	6.3	25	16.9
		56	0.051	6.2	25	20.0

Table 3. Average corrosion rates (mmpy) in coupon after 14, 28, 42 and 56 days

	Low-Carbon Steel Coupon				**Stainless Steel 304 Coupon**			
Days	14	28	42	56	14	28	42	56
Sandy soil	0.87	0.80	1.67	1.54	0.15	0.04	0.06	0.07
Silt soil	1.47	1.74	1.87	2.56	0.08	0.06	0.08	0.09

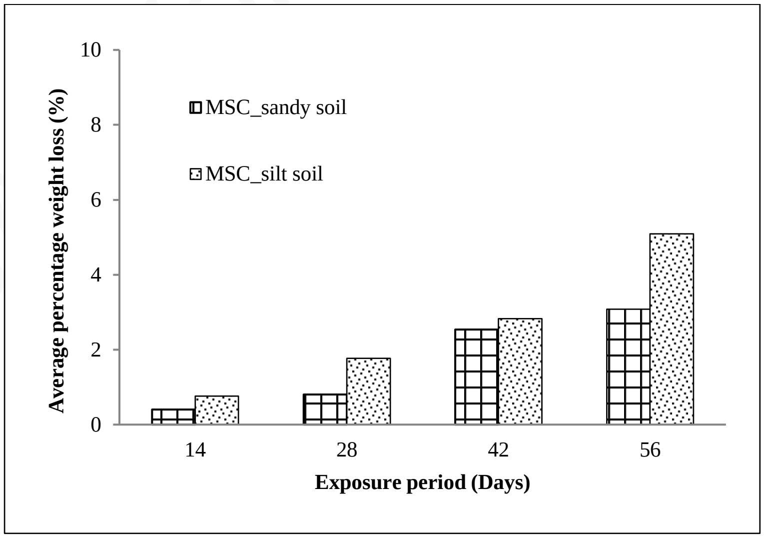

Figure 5. Average percentage weight loss in LCS coupons from sandy soil and silt soil sites

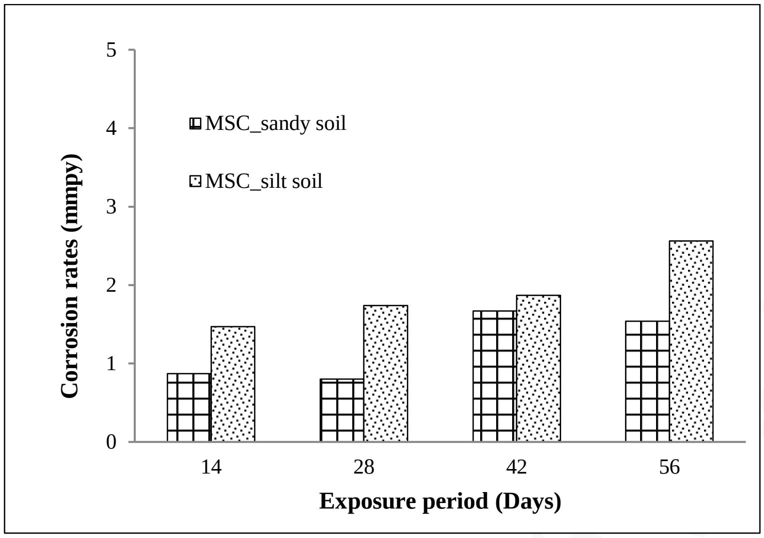

Figure 6. Corrosion rates in LCS coupons from sandy soil and silt soil sites

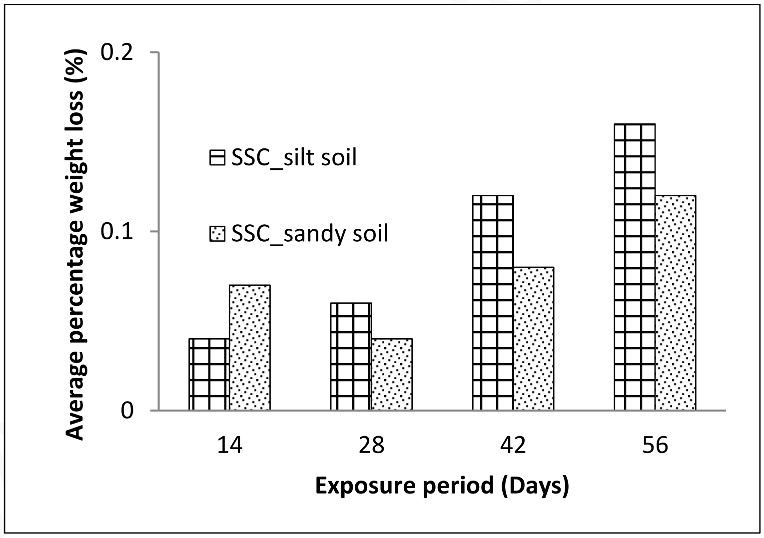

Figure 7. Percentage weight loss in SS 304 coupons from sandy soil and silt soil sites

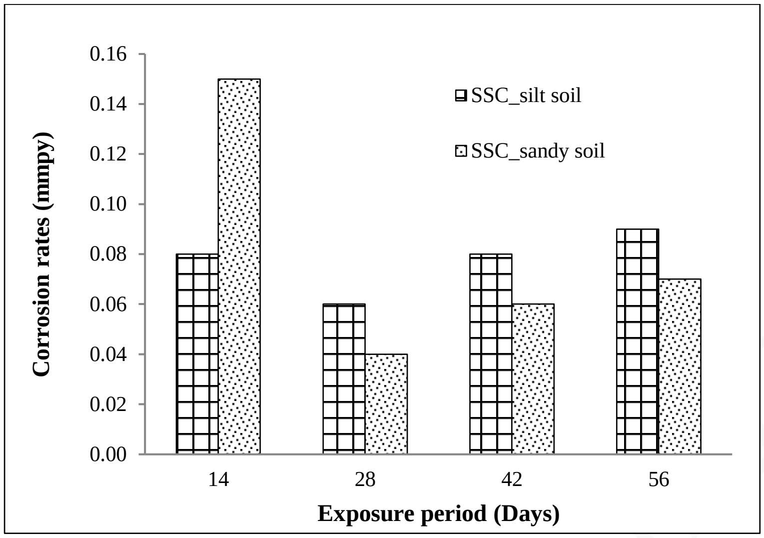

Figure 8. Corrosion rates in stainless steel 304 coupons from sandy soil and silt soil sites

Potentiodynamic polarization

The cathodic and anodic potentiodynamic polarization (PP) curves for both LCS and SS 304 in the studied soils with different conditions of the different exposure periods and at ambient temperature (30 ± 1 ◦C) for sandy soil and at ambient temperature (24 ± 1 ◦C) for silt soil. The corrosion rate can be calculated from the icorr values of LCS and SS 304 in the studied soils at different *in-situ* parameters. The PP parameters for the corrosion of both steels in the studied soils are recorded in Table 4. The value of anodic and cathodic Tafel lines (βa and βc) shows the changes of anodic and cathodic reaction for both metals in both soils. The value of βa for LCS is higher in silt soil than sandy soil due to the metals' anodic dissolution process.

Meanwhile, the value of βc for both metals in sandy soil is lower than silt soil due to the lower oxygen diffusion rate. For both sandy soil and silt soil studied, E_{Corr} values were shifted to more negative values with increasing soil moisture content, indicating that the corrosion process has occurred with predominantly affected by the cathodic reaction. Similar behavior was reported elsewhere [12]. Corrosion current density (i_{Corr}) value shows a higher trend in silt soil than sandy soil. This is due to the higher ionic migration in silt soil due to the ionic conduction path provided by the moisture content in contrast to sandy soil. The corrosion rate of both metals in silt soil is also higher than sandy soil as the metals' corrosion rate is directly proportional to the i_{Corr} value.

Electrochemical impedance spectroscopy

EIS was used to investigate the effect of moisture content of the studied soils on the electrochemical behavior of LCS and SS 304 at ambient temperature. It is well known that the interpretation of EIS data largely depends on the development of equivalent circuits at the metal/electrolyte interface. The Nyquist plot for LCS and SS 304 in sandy soil and silt soil were depicted in Figure 9 - 12, respectively.

It was found that the shape of the plot represented by one semicircle due to the single time constant represented by all studied samples. A bigger semicircle is associated with better charge transfer resistance at the electrode-electrolyte interphase [13]. The value of charge transfer resistance R_{ct} in Table 5 shows that LCS and SS 304 in sandy soil have a higher value than LCS and SS 304 in silt soil. It is inferred that sandy soil provides more impedance towards corrosion activity. This is due to the lower charge transfer process occurs at the LCS and SS 304 surface with the electrolyte.

Meanwhile, silt soil shows lower charge transfer resistance due to its nature that contained higher soil moisture, consequently facilitating the ignition of the corrosion process. The deviation from the ideal semicircle (the time constant dispersion) was also attributed to the inhomogeneities of the electrode surface [14]. However, in all studied cases, the system response in the Nyquist complex plain is an incomplete semicircle whose diameter and shape depend on the soil types and moisture content.

Scanning electron microscopy

Figure 13 - 16 depict SEM micrographs after 28 days of exposure to the sandy soils with different magnifications to see the pattern of the type that occurred on the steel surface.

Figures 13 - 20 depict SEM micrographs after 56 days of exposure to the sandy soil with different magnifications to see the pattern of the type that occurred on the steel surface.

Scanning electron microscopy (SEM) was used to observe the nature of deterioration of the test coupons. All micrographs show the surface features of the studied coupons after treatment with the cleaning solution. SEM was subjected to the surface of LCS and SS 304 after 28 days and 56 days of exposure to the sandy soil. The attachment of sediment products can be observed through SEM. The analysis of SEM confirms corrosion rates that happen to the surface of the steel coupons, and the type of corrosion that occurs on the steel surface can be observed through SEM.

SEM observed that the damage causes generally represent LCS by general corrosion, while SS304 surface damage was mainly due to the pitting corrosion. LCS surface damage is faster based on the image from the test due to the steel composition. The corroded area of LCS was found to be higher than the SS 304. The depth of the pitting that occurred was the same at all over the surface. SS 304 is resistance to corrosion compared to LCS. This argument is fixed with the result published by Wasim et al. [15] on their study reported that mild steel has more damage than the stainless steel at both sandy soil and silt soil due to the steel composition and their properties whereas mild steel is resistant to corrosion. Noor et al (2018) stated that the corrosivity of a particular soil could be related to the interaction of soil resistivity, salts in the soil, moisture content, pH, and elemental composition of the soil [16].

Table 4. Potentiodynamic polarization parameters of LCS and SS 304 in sandy soil and silt soil

Soil type	**Material**	**Parameter**				
		βc/Vdec^{-1}	**βa/Vdec^{-1}**	**E_{Corr}/V**	**i_{Corr}/mA**	**Corr. Rate/mmpy**
Sandy soil	LCS	0.79154	1.3772	-0.4929	1.64	19.061
	SS 304	1.3747	1.3304	-0.4582	0.3668	4.2625
Silt soil	LCS	0.76756	1.5054	-0.4929	1.77	20.575
	SS 304	2.073	0.46025	-0.4919	1.455	16.907

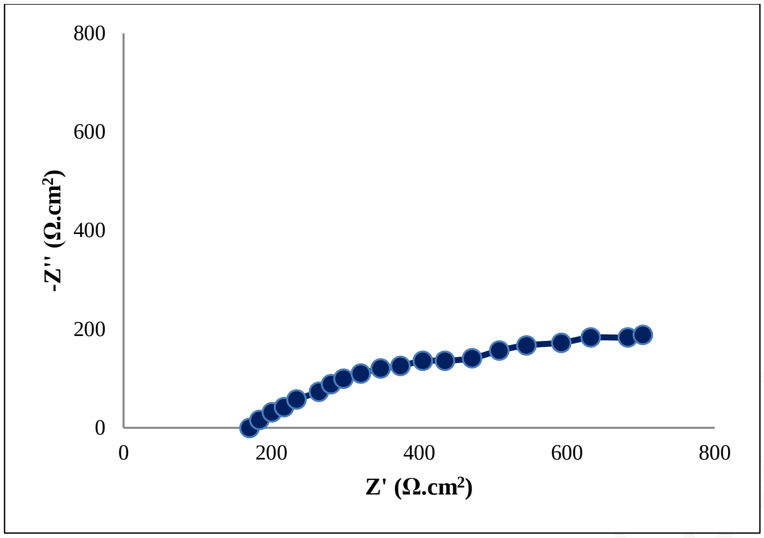

Figure 9. Nyquist plot for LCS in sandy soil

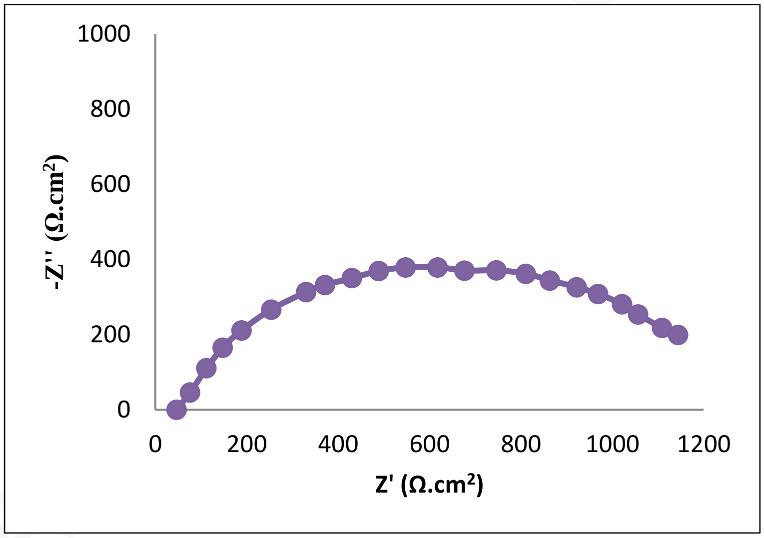

Figure 10. Nyquist plot for SS 304 in sandy soil

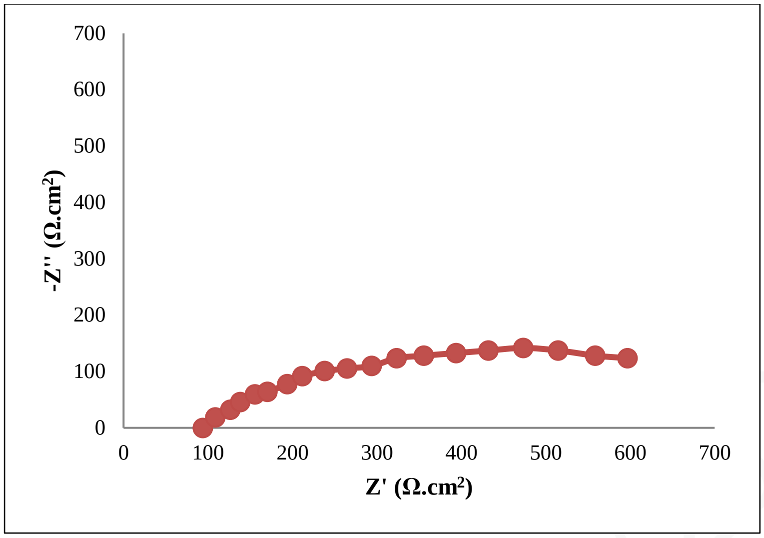

Figure 11. Nyquist plot for LCS in silt soil

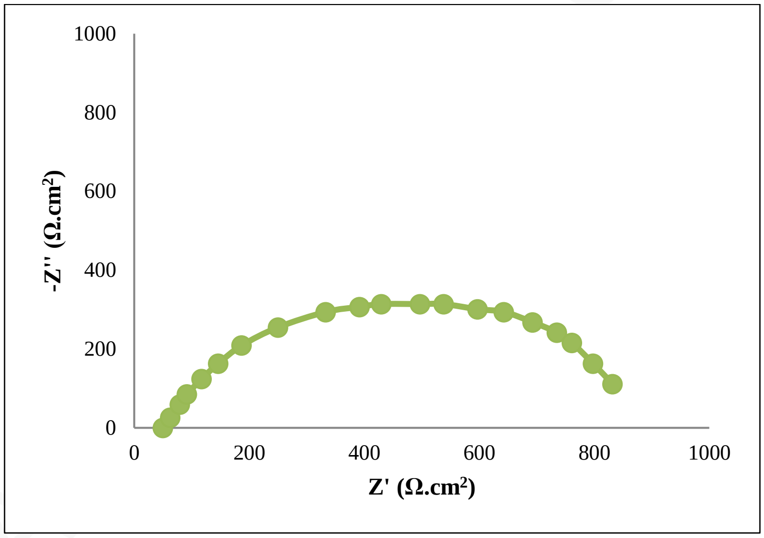

Figure 12. Nyquist plot for SS 304 in silt soil

Table 5. Solution and charge transfer resistance of LCS and SS 304 in sandy and silt soil

Soil	**Material**	R_s **(Ω.cm^2)**	R_{ct} **(Ω.cm^2)**
Sandy	LCS	170.7	801
	SS 304	46.9	1349
Silt	LCS	94.1	712
	SS 304	50.2	899

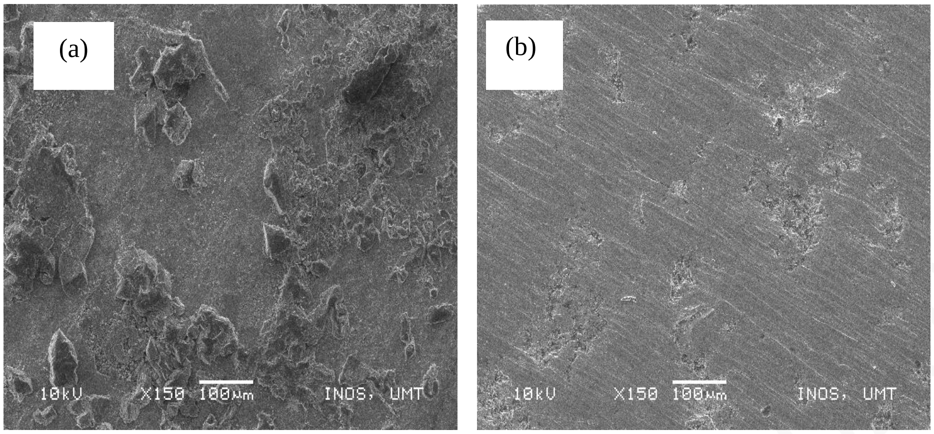

Figure 13. Surface morphology with x150 100μm magnificient of (a) LCS and (b) SS 304, respectively

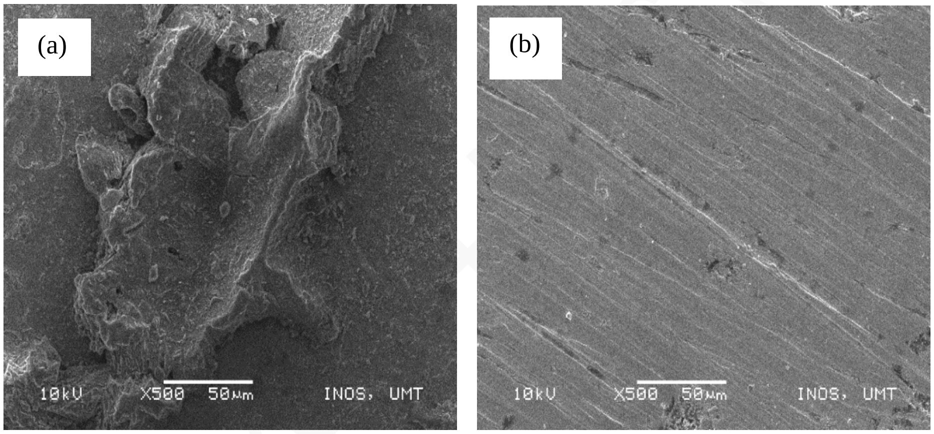

Figure 14. Surface morphology with x500 50μm magnification of (a) LCS and (b) SS 304, respectively

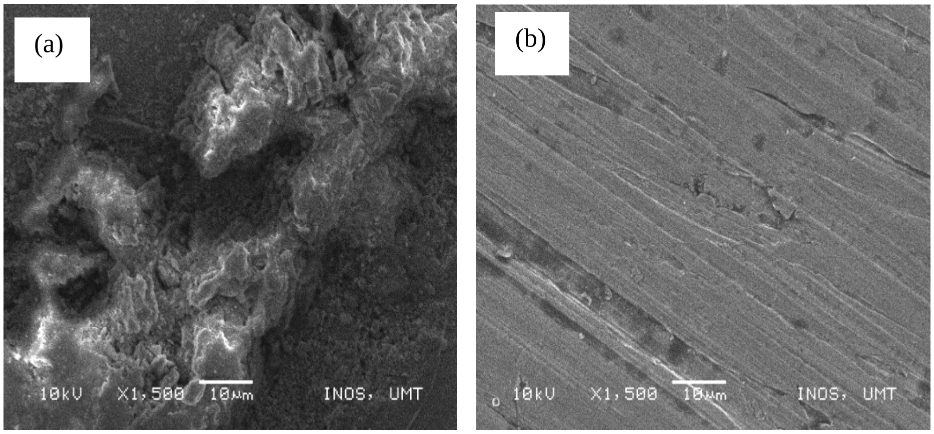

Figure 15. Surface morphology with x1,500 10μm magnification of (a) LCS and (b) SS 304, respectively

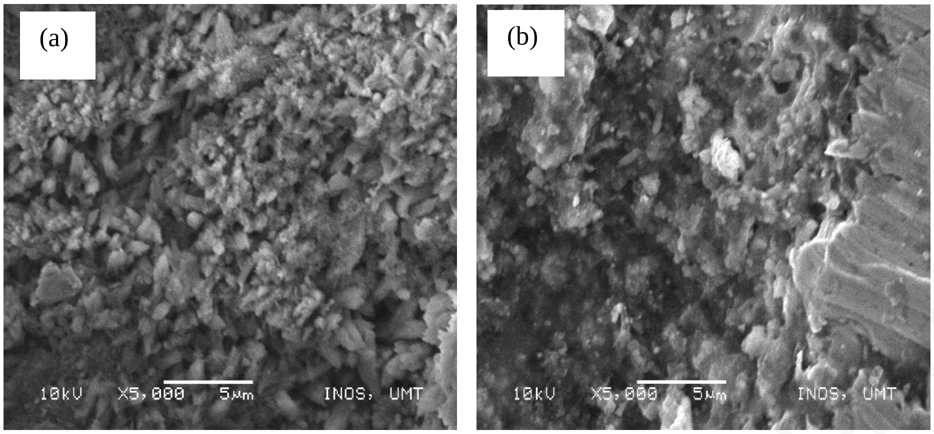

Figure 16. Surface morphology with x5,000 5μm magnification of (a) LCS and (b) SS 304, respectively

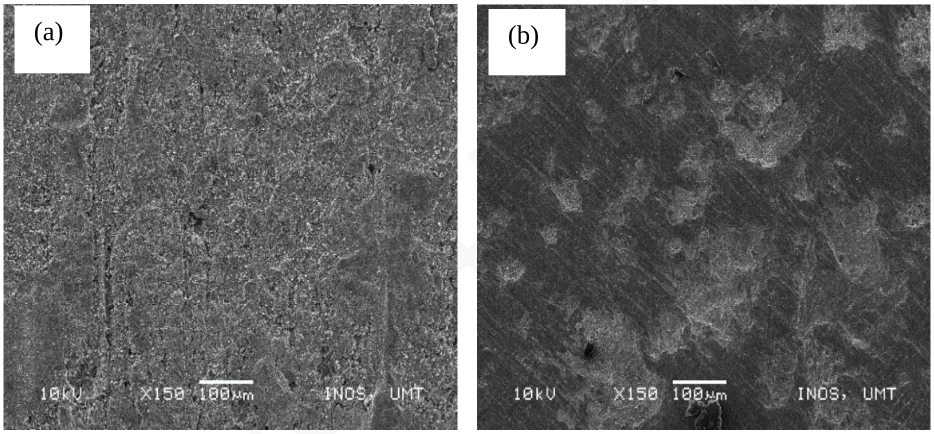

Figure 17. Surface morphology with x150 100μm magnification of (a) LCS and (b) SS 304, respectively

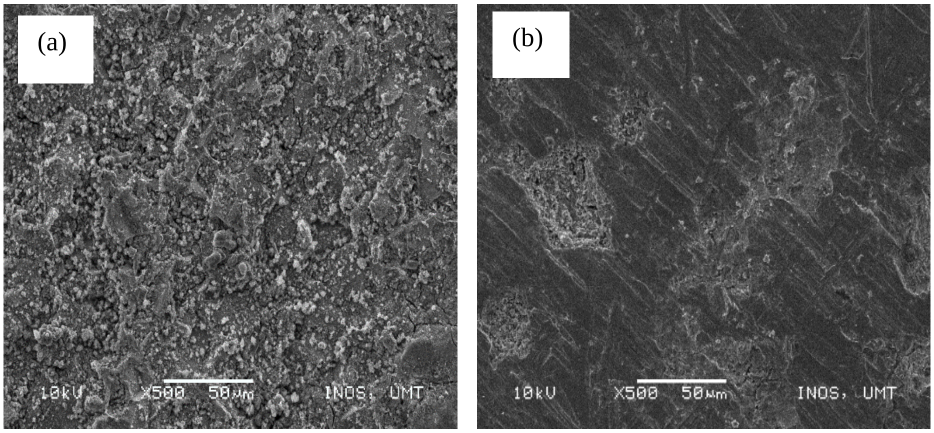

Figure 18. Surface morphology with x500 50μm magnification of (a) LCS and (b) SS 304, respectively

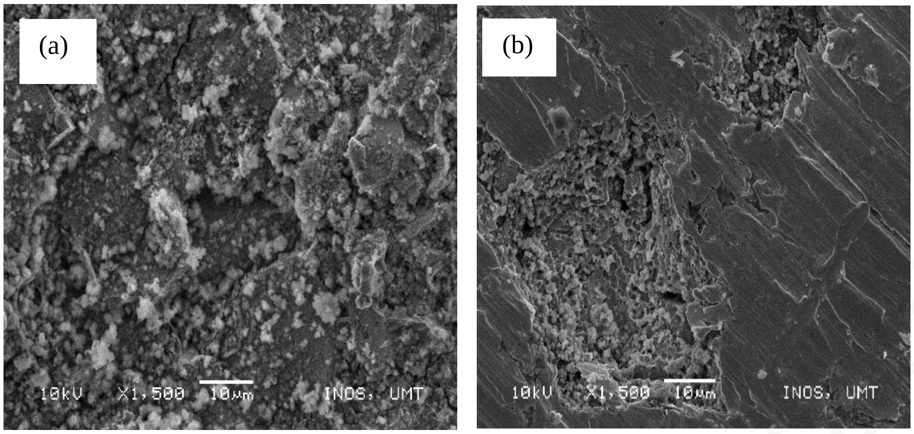

Figure 19. Surface morphology with x1,500 10µm magnificationof (a) LCS and (b) SS 304, respectively

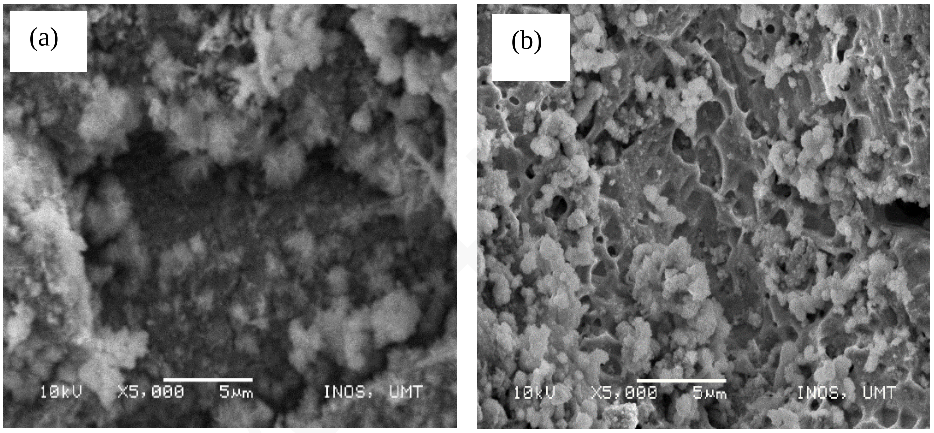

Figure 20. Surface morphology with x5,000 5µm magnification of (a) LCS and (b) SS 304, respectively

Conclusion

This study was conducted to scrutiny the corrosion behavior of LCS and SS 304 buried in two different soils, and it can be concluded that moisture content is the most influential factor on metal loss, whereas pH is relatively insignificant on underground corrosion. The electrochemical analysis shows that the value of E_{corr}, shifted to more negative values following the increment of soil moisture content, indicating that the cathodic reaction predominantly controls the corrosion process. Pitting corrosion and general corrosion occurred on both metal surfaces and both soil types. The pitting area of LCS is larger than the SS 304, and the depth of the pitting that occurred was the same across the surface. The pits area and its distribution on the metal surface also depend on the soil conditions.

Acknowledgment

The authors would like to thank all the members of CoREG (Composites Research Group) UMT, technicians, and support staff from Maritime Technology Lab, UMT, Biocomposite Lab, and INTROP and Advanced Engineering Materials and Composites Research Centre, UPM for their significant contribution and helps.

References

1. Spark, A., Cole, I., Law, D. and Ward, L. (2016). The effect of peptide-based nutrients on the corrosion of carbon steel in an agar-based system. *Corrosion Science*, 110: 174-181.
2. Yan, M., Sun, C., Xu, J. and Ke, W. (2015). Electrochemical behavior of API X80 steel in acidic soils from Southeast China. *International Journal of Electrochemical Science*, 10: 1762-1776.
3. Wu, T., Yan, M., Zeng, D., Xu, J., Sun, C., Yu, C. and Ke, W. (2015). Stress corrosion cracking of X80 steel in the presence of sulfate-reducing bacteria. *Journal of Materials Science & Technology*, 31(4): 413-422.
4. Qin, F., Jiang, C., Cui, X., Wang, Q., Wang, J., Huang, R. and Peng, P. D. (2018). Effect of soil moisture content on corrosion behavior of X70 steel. *International Journal of Electrochemical Science*, 13: 1603-1613.
5. Esfahani, M. N., Coupland, J. and Marimuthu, S. (2014). Microstructure and mechanical properties of a laser welded low carbon–stainless steel joint. *Journal of Materials Processing Technology*, 214(12): 2941-2948.
6. Mobin, M. and Aslam, R. (2018). Experimental and theoretical study on corrosion inhibition performance of environmentally benign non-ionic surfactants for mild steel in 3.5% NaCl solution. *Process Safety and Environmental Protection*, 114: 279-295.
7. Zulkifli, M. F. R., Radzi, N. M., Jusoh, S. M., Saidin, J. and Nik, W. M. N. W. (2019). Potential of cabbage extract (*Brassica oleracea*) as anti-fouling agent in alkyd undercoat for mild steel in seawater. *Malaysian Journal of Analytical Sciences*, 23(3): 451-461.
8. Anwar Ul-Hamida, Huseyin S., Abdul Qudus., Abdulrashid I. M., and Luai M. Al-Hems (2017). Corrosion study of SS304 and SS316 alloys in atmospheric, underground and seawater splash zone in the Arabian Gulf. *Corrosion Engineering, Science and Technology*, 52(2); 134-140.
9. Akkouche, R., Rémazeilles, C., Jeannin, M., Barbalat, M., Sabot, R. and Refait, P. (2016). Influence of soil moisture on the corrosion processes of carbon steel in artificial soil: Active area and differential aeration cells. *Electrochimica Acta*, 213: 698-708.
10. Faes, W., Lecompte, S., Van Bael, J., Salenbien, R., Bäßler, R., Bellemans, I. and De Paepe, M. (2019). Corrosion behaviour of different steel types in artificial geothermal fluids. *Geothermics*, 82: 182-189.
11. Azoor, R. M., Deo, R. N., Birbilis, N. and Kodikara, J. (2019). On the optimum soil moisture for underground corrosion in different soil types. *Corrosion Science*, 159: 108116.
12. Loto, R. T. and Loto, C. A. (2017). Potentiodynamic polarization behavior and pitting corrosion analysis of 2101 duplex and 301 austenitic stainless steel in sulfuric acid concentrations. *Journal of Failure Analysis and Prevention*, 17(4): 672-679.
13. Hajar, H. M., Zulkifli, F., Sabri, M. G, M., Fitriadhy, A. and Nik, W. N. W. (2017). Lawsonia inermis performance as corrosion inhibitor for mild steel in seawater. *International Journal of ChemTech Research*, 9(8): 600-608.
14. Hirschorn, B. D. (2010). Distributed time-constant impedance responses interpreted in terms of physically meaningful properties. Thesis University of Florida.
15. Wasim, M., Shoaib, S., Mubarak, N. M. and Asiri, A. M. (2018). Factors influencing corrosion of metal pipes in soils. *Environmental Chemistry Letters*, 16(3): 861-879.
16. Noor, E. A. and Al-Moubaraki, A. H. (2014). Influence of soil moisture content on the corrosion behavior of X60 steel in different soils. *Arabian Journal for Science and Engineering*, 39(7): 5421-5435.